Dalton Transactions

Halogenation Affects Driving Forces, Reorganization Energies and "Rocking" Motions in Strained $[Fe(tpy)_2]^{2+}$ Complexes

Journal:	*Dalton Transactions*
Manuscript ID	DT-ART-07-2021-002314.R1
Article Type:	Paper
Date Submitted by the Author:	08-Sep-2021
Complete List of Authors:	Kwon, Hyuk-Yong; North Carolina State University, Chemistry Ashley, Daniel; North Carolina State University, Chemistry Jakubikova, Elena; North Carolina State University, Chemistry

ARTICLE

Halogenation Affects Driving Forces, Reorganization Energies and "Rocking" Motions in Strained $[Fe(tpy)_2]^{2+}$ Complexes

Received 00th January 20xx,
Accepted 00th January 20xx

DOI: 10.1039/x0xx00000x

Hyuk-Yong Kwon,†[a] Daniel C. Ashley,†[a,b] and Elena Jakubikova*[a]

Controlling the energetics of spin crossover (SCO) in Fe(II)-polypyridine complexes is critical for designing new multifunctional materials or tuning the excited-state lifetimes of iron-based photosensitizers. It is well established that the Fe–N "breathing" mode is important for intersystem crossing from the singlet to the quintet state, but this does not preclude other, less obvious, structural distortions from affecting SCO. Previous work has shown that halogenation at the 6 and 6" positions of tpy (tpy = 2,2';6',2"-terpyridine) in $[Fe(tpy)_2]^{2+}$ dramatically increased the lifetime of the excited MLCT state and also had a large impact on the ground state spin-state energetics. To gain insight into the origins of these effects, we used density functional theory calculations to explore how halogenation impacts spin-state energetics and molecular structure in this system. Based on previous work we focused on the ligand "rocking" motion associated with SCO in $[Fe(tpy)_2]^{2+}$ by constructing one-dimensional potential energy surfaces (PESs) along the tpy rocking angle for various spin states. It was found that halogenation has a clear and predictable impact on ligand rocking and spin-state energetics. The rocking is correlated to numerous other geometrical distortions, all of which likely affect the reorganization energies for spin-state changes. We have quantified trends in reorganization energy and also driving force for various spin-state changes and used them to interpret the experimentally measured excited-state lifetimes.

Introduction

Spin-state switching is an important and powerful feature of first-row transition metal complexes, particularly when the metal is Fe(II).[1] Changing from the low-spin singlet state to the high-spin quintet state due to changes in temperature, pressure, or light is referred to as spin crossover (SCO) and can potentially be exploited in the development of novel multifunctional materials, quantum computing devices, or spintronics.[2-5] Being able to tune and predict spin-state energetics is also useful for understanding the intersystem crossing (ISC) processes that determine the lifetime of various excited states relevant for photochemical applications of Fe(II).[1, 6] For example, in dye-sensitized solar cells (DSSCs), a metal complex can be used as a chromophore to photochemically form a metal-to-ligand charge transfer state (MLCT) capable of transferring an excited, high-energy electron to a semiconductor to then perform useful work.[7, 8] First studies with Fe(II) complexes as photosensitizers were performed by Ferrere and coworkers, who shown that while in principle Fe(II)-polypyridines are capable of undergoing interfacial electron transfer into the TiO_2 semiconductor upon excitation with visible light, they are much less efficient than their Ru(II) analogues.[9-11] An obstacle to using Fe(II) in these devices, however, is that the initially formed MLCT state is typically short-lived, with most complexes possessing a lifetime on the order of ~100 fs.[12, 13] The shorter this lifetime, the less likely the MLCT state will undergo electron-transfer, and hence this is a major obstacle to constructing efficient DSSCs using an Fe(II) chromophore.[6] The origin of this short lifetime is due to the presence of low-lying high-spin states which provide numerous potential pathways for ISC. The exact mechanism of ISC however, is not known, and there are multiple competing proposals based on varying experimental and computational evidence.[1, 13-21]

Being able to control and design *a priori* the spin-state manifold of Fe(II) would enable much more effective implementation/inhibition of SCO and ISC processes. Tuning the spin-state energetics comes down to understanding what general electronic and structural features are most relevant in determining the potential energy surfaces (PESs) for the relevant spin states. It has long been established that changes in Fe-ligand bond lengths are critical for describing SCO, as changing from one spin-state to another (for example, the ground state singlet to the quintet) involves changes in the population of Fe-ligand antibonding e_g* orbitals, which strongly affects the Fe-ligand bond strengths.[22, 23] Any relevant reaction coordinate for ISC will then naturally incorporate Fe-ligand stretching motions, but this does not mean that this Fe-ligand "breathing" motion is the only relevant structural motion for these processes. For example, torsional "twisting" motions

[a] *Department of Chemistry, North Carolina State University, 2620 Yarbrough Dr., Raleigh, NC 27695, United States.*
[b] *Current Address: Department of Chemistry and Biochemistry, Spelman College, Atlanta, GA 30314, United States.*
†*These authors contributed equally*
Electronic Supplementary Information (ESI) available: Raw calculated energies for all species considered including energies used to calculate reorganization energies (PDF). Cartesian coordinates of all optimized structures, and Cartesian coordinates of all structures along each scan (XYZ). See DOI: 10.1039/x0xx00000x

have been shown to be important in numerous theoretical and experimental studies of trischelate complexes such as $[Fe(bpy)_3]^{2+}$ (bpy = 2,2′-bipyridine).[24-37]

A particularly interesting complex is the bischelate $[Fe(tpy)_2]^{2+}$ (tpy = 2,2′;6′,2″-terpyridine). This complex displays light-induced excited-state spin trapping (LIESST) behavior, in which the complex undergoes ultrafast ISC into a long-lived ^{5}MC upon the visible-light excitation into the manifold of MLCT states.[38] While ^{1}MLCT → ^{5}MC ISC process as well as the relaxation back to the singlet ground state are often interpreted as occurring along the Fe-L symmetric breathing coordinate, several previous studies suggested potential contributions from additional degrees of freedom. For example, Hauser and coworkers argued that a tpy bending mode that involves changes in the angle between the inter-ring bonds of a single tpy ligand is involved in the relaxation pathway between the long-lived ^{5}MC state and the singlet ground state of the $[Fe(tpy)_2]^{2+}$ complex.[39] Another experimental study showed that the ^{1}MLCT → ^{5}MC reaction coordinate does contain structural distortions besides metal-ligand stretching; specifically, that it is best described as a double-axial bending motion.[40] Such distortions were previously also reported for several iron(II) complexes with meridional tridentate ligands.[41-47] In a separate study, an extensive density functional theory (DFT) analysis was performed on this complex to map out its spin-state manifold to determine at what structures do these surfaces cross.[48] One feature that arose from this is that in addition to the Fe-N stretching motions, a gentle "rocking" motion (here denoted as Θ, see Figure 1) provided very energetically flat regions in the vicinity of minimum energy crossing points (MECPs). Furthermore, because this rocking motion arises from a first-order Jahn-Teller distortion, it is associated with the high-spin quintet state, but not the low-energy singlet state, meaning this motion may be part of the reaction coordinate for changing spin state. All together this study demonstrated that rocking is both accessible and relevant for ISC, and that inhibiting this motion, for example by judicious tpy ligand substitutions, may play a role in modifying the PESs along the relevant coordinates and slowing down the ISC.

Recently Damrauer and coworkers have showed that substituting halogens (X) at the 6 and 6" positions of tpy ($[Fe(tpy^X)_2]^{2+}$) dramatically increased the lifetime of the excited MLCT state to 10-20 ps (Figure 1).[49, 50] Substitution also induced significant structural distortions, and changed the spin state energetics, with addition of chlorine and bromine now inducing a quintet ground state, and addition of fluorine causing thermal SCO behavior. Potential explanations for these effects were suggested based on how halogenation might impact the reorganization energies. A subset of these complexes that includes the brominated and chlorinated analogues of $[Fe(tpy)_2]^{2+}$, has been recently subject to a computational study by Li at al. that focused on their electronic structure and UV-vis spectra.[51] While the results did not conclusively determine the reason for differences in their excited-state lifetimes, Li et al. highlighted a slight decrease in the energy gaps between the various spin states going from $[Fe(tpy^{Br})_2]^{2+}$ to $[Fe(tpy^{Cl})_2]^{2+}$. The authors also performed an ETS-NOCV (extended transition state

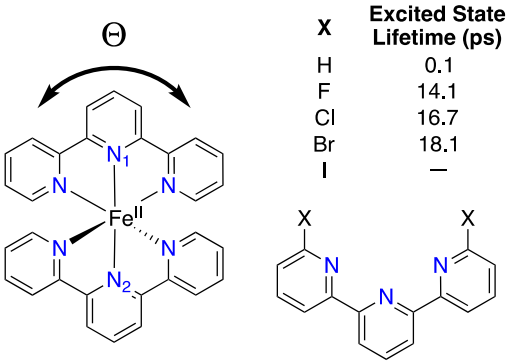

X	Excited State Lifetime (ps)
H	0.1
F	14.1
Cl	16.7
Br	18.1
I	—

Figure 1. Complexes considered in this study along with their experimentally determined excited state lifetimes when available. The tpy rocking coordinate Θ is defined as the angle between the N_1-Fe-N_2 atoms of the $[Fe(tpy^X)_2]^{2+}$ complexes.

energy decomposition analysis combined with natural orbitals for chemical valence) suggesting that substitution with bulky substituents, such as Br, decreases the electrostatic attraction between the metal and ligands relative to the chlorinated complex.

Following up on the work of Damrauer and coworkers, we employ the tools of DFT and TD-DFT to evaluate how halogenation impacts the potential energy surfaces of substituted $[Fe(tpy^X)_2]^{2+}$ complexes (X = H, F, Cl, Br, I), as well as their spin-state energetics and reorganization energies for light-induced spin-state conversion from the initially-excited ^{5,7}MLCT states of the halogenated complexes to ^{3}MC state (^{1}MLCT to ^{3}MC transition in case of the unsubstituted complex). The results show that halogenation has a significant effect on the degree of rocking and the spin-state energetics, the latter being in good agreement with experiment. Analysis of the reorganization energies and thermodynamics support the proposal that a triplet intermediate is important in the ISC cascade.

Since the original analysis by Damrauer and coworkers did not focus on interpretation of how spin-orbit coupling (SOC) affects the light-induced dynamics of these complexes, but focused on the evaluation of the reorganization energy and the driving force for these processes, we also emphasize the same issues here as our goal is to provide a computational perspective on the original experimental interpretations. Regardless, it is well known that SOC can be critical for description of intersystem crossing processes.[52] Therefore, we consider this work to be only an initial step toward building a complete computational model of this system.

Computational Methodology

Structure Optimization

All structures were optimized in vacuum with the B3LYP[53-56] functional including Grimme's D2 dispersion correction[57] (B3LYP+D2), unless noted otherwise. In the previous study with Fe(II) polypyridine complexes,[58] B3LYP+D2 showed the average percent error in the metal-ligand bond lengths of 2%, and showed very similar performance of spin-state energetics to B3LYP*[54, 59-61] which was specifically reparametrized to

reproduce spin-state energetics of iron pseudo-octahedral complexes. The SDD basis set and accompanying pseudopotential were used for Fe[62] and I,[63] and the 6-311G* basis set was used for all other atoms.[64] An ultrafine integral grid was used for all calculations. Frequencies were calculated for all optimized structures using the harmonic oscillator approximation to verify the nature of the stationary points. The results of these frequency calculations were also used to calculate zero-point energy and entropic corrections to the free energies at 298.15 K and 1.0 atm using standard statistical mechanical conventions. Solvation effects were incorporated implicitly using the IEF-PCM formalism with water as the chosen solvent. Stability calculations were performed for all constrained optimizations evaluated on rocking PESs. Any unstable wavefunctions were optimized and the resulting stable wavefunction was then used as the initial guess for a new geometry optimization. All calculations were performed with the Gaussian 09 electronic structure package.[65]

Spin-State Energetics

The calculations of high-spin vs low-spin energy differences ($\Delta E_{HS/LS}$) with DFT are known to be less reliable unless the functional parameters are calibrated for a specific family of complexes.[66-68] To check the reliability of the DFT methodology, the exact-exchange scan was performed for the interested complexes (see SI Figure S1).[6, 69] The energy differences between ^{1}MC, ^{3}MC, and ^{5}MC for investigated complexes are almost linear and parallel with the change in the exchange coefficient suggesting the spin-state energetics comparison between the complexes are internally consistent. ^{7}MLCT energy is also linear relative to ^{5}MC energy, but not as parallel. This results in the change in energy ordering between the two spin states based on the complex and functional used. However, for both B3LYP (20%) and B3LYP* (15%), the order of $\Delta E_{HS/LS}$ by each complex is consistent for all spin-states. These benchmarks suggest that while absolute energies calculated with our chosen methodology may not be reliable, we should be able to draw conclusions from the comparison of the calculate relative energy differences across the series of complexes investigated in this work.

Driving force and reorganization energies

In this study, it was important to calculate thermodynamic terms relating to interconversion of various spin states. These were the driving force (ΔG) and the reorganization energy (λ), the latter term originating from the Marcus theory for electron transfer.[70, 71] While Marcus theory was not derived to describe spin state changes, it has been employed to investigate the ISC processes previously.[72] Furthermore, the reorganization energy was used to explain Damrauer and coworkers' results,[50] therefore we have investigated it here as well. Calculating ΔG between the minima of different spin states was trivial, but λ was not. Figure 2 shows two different ways in which λ can be calculated. Calculating λ starting from the reactant,[71] referred to here as λ(R), is done by subtracting the optimized reactant energy from a single point energy calculation done with the reactant spin state at the product geometry. Alternatively, λ can be calculated from the product,[73] referred to here as λ(P), which is done by subtracting the optimized product energy from a single point energy calculation done with the product spin state at the reactant geometry. Averaging the two values calculated in this manner is essentially Nelson's 4-point method.[74-76] Both definitions appear occasionally in the literature and they are at times used without distinction.[77] This is because in the standard derivation of the Marcus equations λ(R) and λ(P) are identical, since the reactant and product surfaces are modeled as parabolas with equivalent curvatures. Note this is not necessarily indicating that the reactant and product surfaces actually have equivalent curvatures, but rather that they are modeled with the same reduced force constant: $k = 2k_rk_p/(k_r+k_p)$.[71]

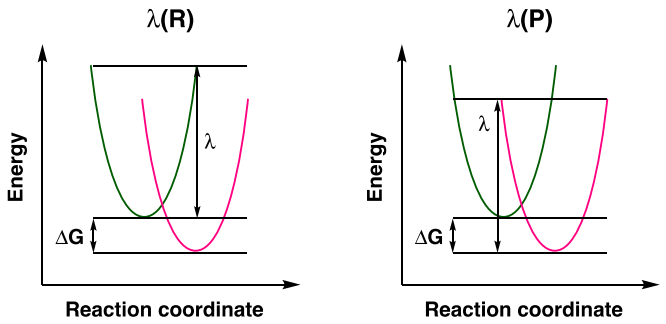

Figure 2. Different ways to calculate λ, either starting from the reactant (left) or the product (right).

Direct calculations of the two terms, λ(R) and λ(P), will not be equivalent, however, if the curvature of the reactant and product surfaces are not identical. A typical solution is to average the values, as mentioned above, and this arithmetic mean of λ(R) and λ(P) will be referred to as λ(A). Recent work[75] has explored what type of averaging is more appropriate, but as our results were generally very similar regardless of whether an arithmetic or geometric mean was calculated, only the former was reported. Much work has been done in asymmetric Marcus-Hush theory,[78] where often the different curvature of the reactant and product surfaces is directly included, but again it is not necessarily straightforward to apply these formalisms to the present situation as here we are explicitly calculating reorganization energies for spin-state changes as opposed to modeling them for electron-transfer. From the standpoint of considering λ's influence on the interconversion from reactant to product, it would seem that λ(R) should be more relevant, as it directly reflects the reorganization energy starting from the reactant state, just as would happen in the actual reaction. All three values of λ are reported due to these complications. Note that the three terms yield similar, but not identical values (always within a few kcal/mol), although the trends in these values are not always the same.

Result and Discussion

Spin-state Energetics and Quintet Structure

Experimentally it is known that $[Fe(tpy)_2]^{2+}$ is a ground-state singlet. Halogenation at the 6 and 6" positions with chlorine or bromine was observed to change the ground state to the quintet, while fluorination produced thermal SCO behavior (singlet at low temperatures and quintet at high temperatures).[49, 50] The first step in the DFT analysis of these complexes was to determine if the methodology was able to reproduce these observations. The spin states of interest are shown in Figure 3 and the calculated spin-state energetics are given in Table 1. The calculations predicted that electronically the unsubstituted complex $[Fe(tpy)_2]^{2+}$ prefers the singlet state to the quintet by 5.5 kcal/mol, while the chlorinated and brominated complexes prefer the quintet state to the singlet by ~11 kcal/mol. Furthermore, for the fluorinated complex the singlet and quintet are within ~3 kcal/mol of each other, which is what would be expected for a complex capable of thermal SCO. Although no experimental data was available for the iodinated complex, its calculated spin-state energetics were similar to its brominated analogue. Finally note that for each complex the triplet state is always 10-15 kcal/mol higher in energy than the ground state.

Importantly, while the electronic energies all successfully reproduce the observed ground states, inclusion of thermal and entropic effects to calculate relative free energies does not agree as well. As expected, the higher spin states are further stabilized entropically and as such the quintet states (amongst others) becomes lower in energy.[1] This causes the singlet and quintet states of the unsubstituted complex to become isoenergetic, and to become significantly separated in energy for the fluorinated complex. The calculations, however, do successfully reproduce the experimental trends in the relative energies of the quintet and singlet states when comparing the complexes to each other, which is more important for the current study than absolute accuracy in predicting the spin-state ordering.

It was also important to consider the relevant MLCT state. While this state is likely, at least initially, a quintet state for the halogenated complexes due to arising from the quintet ground state, a ^{5}MLCT state is difficult to model at the same level of theory. Because the ^{5}MLCT is so much higher in energy than the metal-centered quintet (^{5}MC), the ^{5}MLCT is highly prone to immediately collapsing to the ^{5}MC state during the SCF procedure. If it is assumed that the coupling between the ligand-based electron and the metal-based electrons is relatively weak, then the heptet (^{7}MLCT) can also be considered a relevant model for the MLCT state (see Figure 3). This is a reasonable assumption in the same way it is expected that the ^{3}MLCT and ^{1}MLCT states may both be accessible after exciting from a singlet (^{1}MC) state in more typical Fe(II) polypyridine complexes. Note that the splitting between the ^{3}MLCT and ^{1}MLCT states in a related $[Fe(bpy)_3]^{2+}$ complex was previously calculated to be relatively small, on the order of 0.1 to 0.2 eV, and both of these states can be plausibly involved in the excited-state decay pathways.[52, 79] Therefore, the ^{7}MLCT state was optimized as well. As expected, it was much higher in energy than the other spin states, on the order of ~50 kcal/mol higher than the ^{5}MC state.

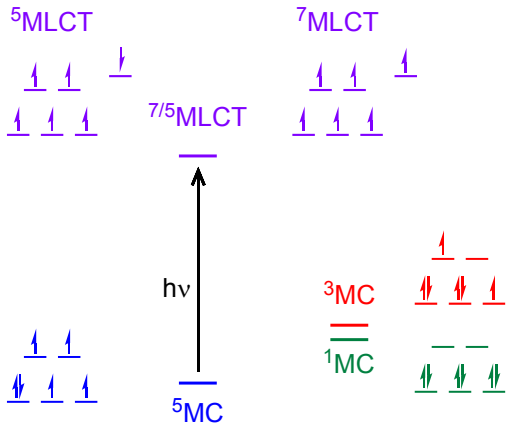

Figure 3. Qualitative illustration of the spin states of interest and their orbital occupations, specifically drawn for the complexes which assume a ^{5}MC ground state.

Table 1 shows that halogenation increases the lifetime of the MLCT excited state by an order of magnitude. There is also a trend amongst the halogenated complexes, where on increasing the size of the halogen the lifetime steadily increases. Note that there is a larger increase of lifetime on going from fluorine to chlorine then there is going from chlorine to bromine (2.6 vs. 1.4 ps). The focus of much of this study was examining energetic and structural parameters of these complexes to see what features may be responsible for these specific trends in lifetime. As mentioned earlier, the rocking angle of the ^{5}MC state was of particular interest based on its importance determined in an earlier study.[48] Figure 4 shows the optimized structures of the ^{5}MC states for each complex. As the size of the

Table 1. Calculated spin-state energetics (in kcal/mol), experimentally determined ground states, and experimentally determined excited state lifetimes for $[Fe(tpy^X)_2]^{2+}$.[49, 50] The numbers in parentheses are relative free energies i.e. they include ZPE and entropic corrections.

ΔE (ΔG)	H	F	Cl	Br	I
^{5}MC	0.0 (0.0)	0.0 (0.0)	0.0 (0.0)	0.0 (0.0)	0.0 (0.0)
^{3}MC	9.7 (11.0)	11.8 (13.9)	13.3 (13.7)	14.0 (15.8)	14.4 (14.5)
^{1}MC	-5.5 (0.0)	2.8 (9.1)	10.5 (14.1)	12.1 (16.8)	13.3 (16.5)
^{7}MLCT	43.7 (42.3)	50.5 (49.4)	53.7 (52.8)	54.2 (54.7)	55.4 (54.2)
Ground state (experimental)	Singlet	SCO	Quintet	Quintet	--
Lifetime (ps) (experimental)	0.1	14.1	16.7	18.1	--

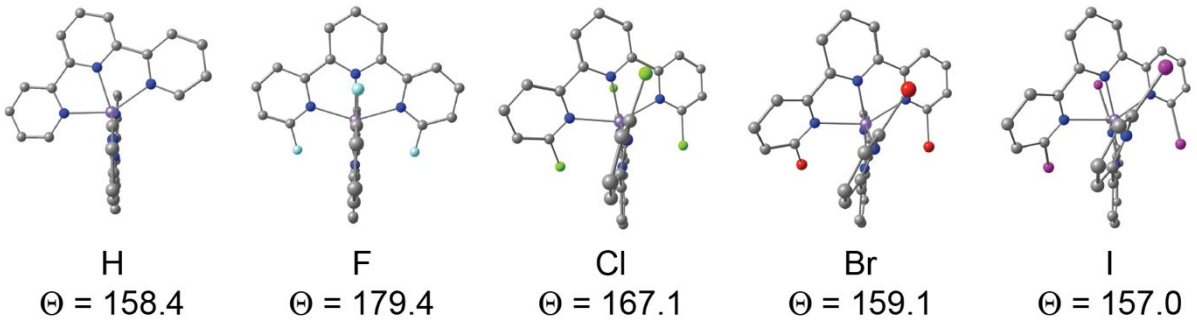

Figure 4. Optimized structures for the ^{5}MC state of $[Fe(tpy^X)_2]^{2+}$. The rocking angle (Θ) is given in degrees for each structure.

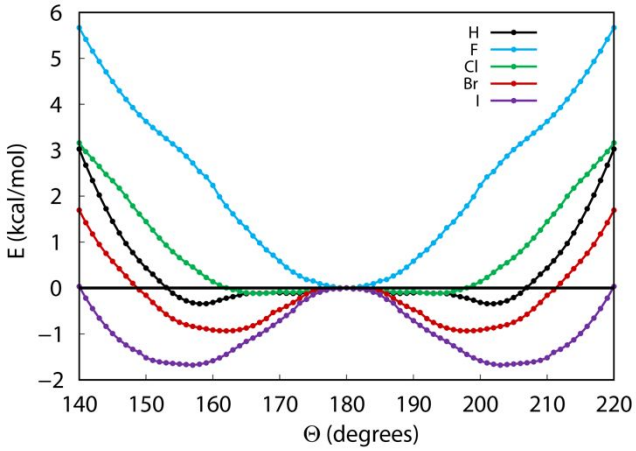

Figure 5. Rocking PESs for the ^{5}MC state of $[Fe(tpy^X)_2]^{2+}$.

halogens increases, the rocking angle successively increases, from no rocking for the fluorinated complex to the heavily rocked iodinated complex. Interpreting these trends purely in terms of size seems obvious, as the larger halogens will cause greater inter-ligand repulsion leading to further rocking. Speaking against this, however, is the unsubstituted complex, which is significantly rocked, in fact it has a calculated rocking angle similar to the brominated complex (158.4° vs. 159.1°, respectively) despite hydrogen being similar in size to fluorine. This suggests that trends in the halogenated complexes are not necessarily directly related to the unsubstituted complex.

Potential Energy Surfaces for the Rocking Motion

More insight can be gleaned by calculating the one-dimensional potential energy surfaces (PESs) corresponding to this rocking motion for the ^{5}MC state, as shown in Figure 5. The surfaces themselves are consistent with the structures presented in Figure 4, namely that the previously reported rocking angles correspond to the minima indicated on the scans. The scans also give an indication of the energetic penalty incurred upon rocking the tpy^X ligand. Notably, the fluorinated complex has the steepest potential by far, with a rock of 40 degrees raising the energy by ~6 kcal/mol. As the halogen becomes larger, the surface becomes flatter, and the minimum at 180 degrees becomes a maximum while the minima now lie at increasingly rocked positions, just as shown in Figure 4. For the chlorinated and brominated structures, the "barrier" for rocking back and forth will be less than 1 kcal/mol, and for the iodinated structure is still less than 2 kcal/mol. The unsubstituted parent complex also has a very flat surface, as previously reported in the earlier PES work.[48] As mentioned before, the shape of this surface appears to be in between the chlorinated and brominated structures. The calculated surfaces strongly suggest that while halogenation causes significant and predictable changes in the shapes of the rocking PESs, rocking is still an accessible motion and can potentially be important for ISC. The one possible exception to this is for the fluorinated complex, where the surface is relatively steeper.

The ^{7}MLCT state rocking PESs qualitatively shows some similarities to the ^{5}MC state, for example the preferred degree

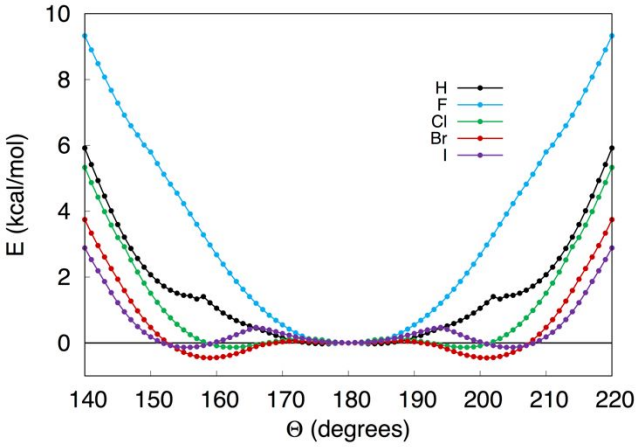

Figure 6. Rocking PESs for the ^{7}MLCT state of $[Fe(tpy^X)_2]^{2+}$.

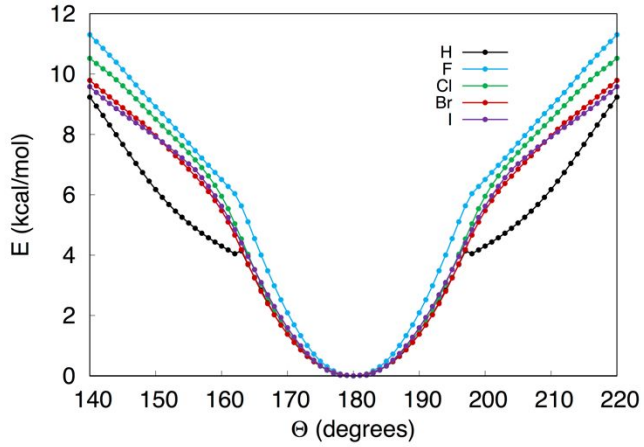

Figure 7. Rocking PESs for the ^{3}MC state of $[Fe(tpy^X)_2]^{2+}$.

of rocking increases going down the group for each spin state, however the ^{7}MLCT PESs are somewhat steeper (Figure 6). This is consistent with the ^{7}MLCT state having a similar electron configuration (see Figure 3) and a formally higher oxidation state on Fe (III vs. II) than the ^{5}MC state. The ^{7}MLCT states did show other differences as well, namely that while the ^{5}MC scans show minima appearing to either side of the unrocked center, the ^{7}MLCT scans show an additional barrier for forming the rocked minima. While this barrier is very small (it is largest for the iodine complex at ~0.5 kcal/mol relative to the unrocked center), it is nevertheless an interesting qualitative feature. It is important to note that for both the ^{5}MC and ^{7}MLCT states, the fluorinated complex has a significantly steeper rocking potential than all the other considered complexes. Interestingly, this was not the case for the triplet (^{3}MC) states (Figure 7), where all of the halogenated complexes showed almost identical rocking surfaces. The rocking surfaces of the ^{3}MC states are also much steeper than the ^{5}MC and ^{7}MLCT states, which is unsurprising given the lower occupation of e_g* antibonding orbitals.

As show in Figure 7, the unsubstituted parent complex abruptly changes the curvature of its ^{3}MC surface at larger angles. This happens to a lesser extent on the ^{7}MLCT surface as well. This is likely due to switching between different electronic states (related to the formal Jahn-Teller instability of the ^{3}MC state) at this point in the scans. Note that these effects do not significantly affect any conclusions reached from this data. It is likely that there are other electronic states that are close in energy to the examined surfaces for many of the complexes examined in this study. As it was not possible to exhaustively consider every single electronic state for each complex and spin state, only the lowest energy state (based on stability analysis) at a given geometry was considered.

While the rocking angle was the main interest in this study, it is important to keep in mind that rocking is but one feature of a multidimensional PES, and that it can be coupled to other structural distortions that may be equally or more important for ISC, such as intraligand distortions of the tpy ligand as previously suggested by Hauser et al.[39] For the halogenated complexes, it is abundantly clear that the highly rocked structures also show significant intraligand distortions, namely that the three pyridyl rings of each tpy^X are now significantly rotated out of the plane from each other. This rotation has been quantified by taking the sum of the magnitude of these rotations; i.e. the deviations in dihedral angle from 0 degrees, and this value is referred to as "warping". Figure 8 shows the calculated warping at each point along the ^{5}MC 1-D rocking PESs presented in Figure 5. The total warping of fluorinated and unsubstituted complexes is smaller than the other complexes due to the smaller size of the atom having less steric effects against the other ligand in the molecule. For the iodinated and unsubstituted complexes, the degree of warping stays relatively constant throughout the surface, and appears unconnected to rocking. The fluorinated, chlorinated, and brominated complexes, however, show strong coupling of warping with rocking. This highlights that while 1-D PES slices such as Figures 5-7 can provide meaningful information, it is critical to not over interpret them either, as they also reflect other motions coupled to the reaction coordinate being probed (rocking being probed in this case).

Table 2. Calculated thermodynamic parameters for substituted $[Fe(tpy)_2]^{2+}$ complexes considered in this study. All values are given in kcal/mol.

	$^7MLCT \rightarrow {}^3MC$			
X	ΔG	λ(R)	λ(P)	λ(A)
H	-31.3	8.8	9.7	9.3
F	-35.6	7.8	8.2	8.0
Cl	-39.1	6.4	11.7	9.1
Br	-38.8	6.5	12.7	9.6
I	-39.6	6.2	13.8	10.0

Understanding Excited-state Lifetimes

Damrauer and coworkers proposed that the halogenated $[Fe(tpy^X)_2]^{2+}$ complexes are initially excited into a $^{7/5}$MLCT state and this state then decays into a ^{3}MC state before finally relaxing back to the ^{5}MC ground state.[50] The range of lifetime data for $[Fe(tpy^X)_2]^{2+}$ was interpreted based on this mechanism with the assumption that the $^{7/5}$MLCT to ^{3}MC step is rate-determining and that changes in either λ or ΔG for this step are responsible for the decrease in excited state decay rates as the halogens become larger. Using DFT, we have calculated both λ and ΔG terms for this step for each complex and these quantities are given in Table 2. Note that experimentally, the largest increase in lifetime was on changing the F substituent to Cl, with a smaller increase occurring as Cl was changed to Br. Therefore, one would expect to see a more significant change in λ and ΔG going from F to Cl, and a less significant change going from Cl to Br. For the ^{7}MLCT to ^{3}MC conversion ΔG significantly decreases from -35.6 to -39.1 kcal/mol on going from F to Cl, becoming more favorable. The ΔG does not change much between the Cl, Br, and I substituted complexes.

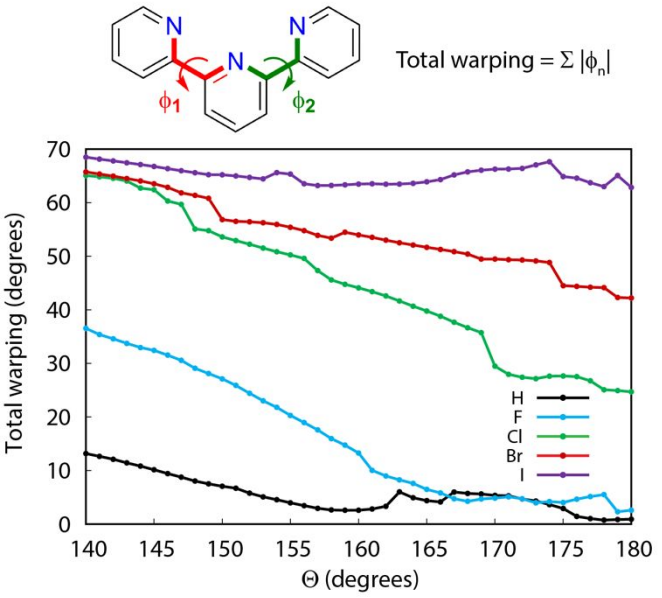

Figure 8. Coupling of warping and rocking motions for the ^{5}MC state in $[Fe(tpy^X)_2]^{2+}$. The rocking angle (Θ) values at fully optimized quintet geometries are as follows: 158.4° (H), 179.4° (F), 167.1° (Cl), 159.1° (Br), and 157.0° (I).

Calculating λ was more complicated. As discussed in the methodology section, there are two non-equivalent ways to calculate λ, depending on whether it is calculated on the reactant (^{7}MLCT) or product (^{3}MC) surfaces, resulting in λ(R) and λ(P), respectively. Reorganization energies obtained via these two different methods would be identical if the curvature of the reactant and product surfaces were identical, but they are not. Although it is physically more reasonable to interpret trends in the forward rate of reaction using λ(R), both terms are considered here. Upon going from F to Cl the λ(R) term gets smaller, going from 7.8 to 6.4 kcal/mol. Like the trend in driving force, λ(R) stays relatively constant for Cl, Br, and I. The trend in λ(P) is different, however: there is an increase in reorganization energy on going from F to Cl, and then a smaller increase going to the heavier halogens. The fact that λ(R) and λ(P) give different trends makes them difficult to interpret, unfortunately. Upon averaging the two terms, the trend also shows a modest increase in reorganization energy across the series, similar to λ(P).

The calculated results were then interpreted within the general framework of Marcus theory. This interpretation will be different depending on whether the system lies in the normal regime (λ > - ΔG) or inverted regime (λ < - ΔG) (see Figure 9). Based on our calculations λ is much smaller than - ΔG for each system, a conclusion that holds true regardless of whether λ is calculated as λ(R), λ(P) or the averaged λ(A). For example, in the fluorinated system -ΔG is 35.6 while λ(R) is 7.8 kcal/mol, λ(P) is 8.2 kcal/mol, and λ(A) is 8.0 kcal/mol. For an inverted system, it is predicted that an increase in driving force and decrease in reorganization energy would cause the rate of reaction to decrease. In this case that would lead to the reactant, the ^{7}MLCT state, having a longer lifetime. The thermodynamic effect of this is shown in Figure 9b (the reorganization energy effect is more difficult to show in the same schematic). This then is consistent with the significant increase in driving force calculated for changing the substituent from F to Cl. This is not consistent with the trends in λ(A), which increase as the halogen becomes heavier. This could simply reflect that the changes in ΔG are what dictates the rates for this system, or it could be an indication that the Marcus theory interpretation is not valid here. It is also worth noting that the trend in λ(R) is opposite from the trend in λ(A).

The explanation given above, that makes use of the fact that the crossing from the $^{7/5}$MLCT surface to the ^{3}MC surface occurs in the inverted regime, is different from what was originally proposed by Damrauer and coworkers.[50] It was suggested that an increase in the stiffness (increase of λ) of the $^{7/5}$MLCT surface and/or an increase in the energy of the ^{3}MC surface (increase of ΔG) could have the effect of raising the energy of the crossing point between the $^{7/5}$MLCT and ^{3}MC states. Both of these possibilities are shown schematically in Figure 9a. The higher energy crossing points would then result in slowing the ISC rate down. This explanation is only viable, however, when the system is in the normal regime, where λ > - ΔG, and as explained above our calculations have shown that λ is much smaller than - ΔG. Finally, another thermodynamic-oriented explanation is simply that according to the energy gap law, as the driving force becomes more favorable the rate of ISC will decrease for weakly coupled systems.[80, 81]

It is interesting to connect these results to the 1D rocking PESs discussed earlier. The product surfaces (^{3}MC, see Figure 7) behave similarly for all of the complexes. The reactant surfaces (^{7}MLCT, see Figure 6), however, show much more variation between complexes. Most importantly, the fluorinated complex has the stiffest rocking PES when compared to the other complexes, and would therefore be interpreted to have the largest reorganization energy on the reactant surface, consistent with the calculated λ(R) values as discussed above. Future work will investigate whether this trend in reorganization energy holds true as the dimensionality of the PES is increased.

Finally, it should be noted that none of the above explanations clarify why the halogenated series as a whole has longer excited state lifetimes than the unsubstituted parent complex. This may be the result of the parent complex having a significantly different spin-state manifold than the halogenated complexes (having a ^{1}MC ground state and/or not being a thermal SCO complex, for example). This work also did not consider spin-orbit coupling (SOC) constants between the different surfaces, which will also influence the rates of the ISC events between the initially-excited MLCT and non-photoactive ^{3}MC states. The calculation of SOC constants could further elucidate the differences between the substituted and unsubstituted complexes and will be investigated in future work. Overall, our present study demonstrates the extent to which substituents at 6 and 6'' positions of the tpy ligand deform the PESs along the tpy rocking coordinates, elucidates the changes in the energetic ordering of various MC and MLCT states of the complex, and suggests that the ^{5,7}MLCT to ^{3}MC conversion occurs in the Marcus inverted region.

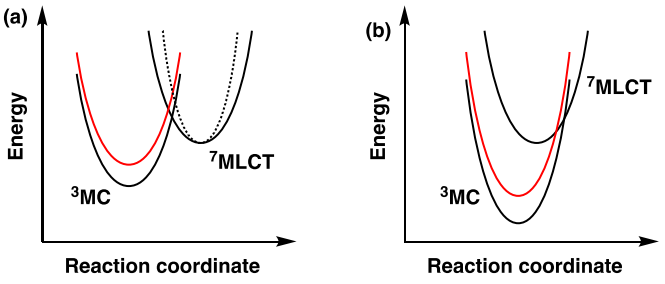

Figure 9. Cartoon illustrating the effect of increasing the energy (red parabola) of the ^{3}MC state on the ^{7}MLCT-^{3}MC crossing for (a) the normal region and (b) the inverted region. The dashed parabola in (a) is to show the effect of increased strain which would manifest as a stiffer parabola. Note the positions on the x-axis are qualitative and the shift of the triplet parabolas in (b) is just to more easily show the inverted crossing.

Conclusions

Utilization of Fe(II) polypyridine complexes as photosensitizers is hampered by their typically short-lived MLCT excited states. Short MLCT state lifetimes arise from rapid ISC due to the presence of low-energy high-spin MC states. Recent experimental work showed that halogenation of $[Fe(tpy)_2]^{2+}$ induced dramatic enhancement of excited state lifetimes, with

these lifetimes increasing as the size of the halogen increases.[49, 50] The DFT calculations presented here further shed light on the possible structural and thermodynamic reasons halogenation has this important effect. Previous computational work has shown that ISC, and spin-state conversion in general, in $[Fe(tpy)_2]^{2+}$ may be connected with a gentle rocking motion of one tpy ligand. Here we see that halogenation has pronounced and predictable effects on the one-dimensional PESs corresponding to this rocking motion. For the ^{5}MC and ^{7}MLCT states, increasing the size of the halogen generally has the effect of increasing the rocking angle and energy stabilization of the rocked minima, likely due to the steric strain that is released by distorting the complex from an ideal octahedral structure. Unsurprisingly, these rocking motions are also coupled to other complex structural distortions, such as intraligand "warping" motions, highlighting the multidimensional nature of ISC. Notably, the fluorinated complex does not show any rocking whatsoever, and has a steep PES, steeper even than the unhalogenated parent complex. The ^{3}MC states, which are believed to be a potential intermediate between the ^{7}MLCT and ^{5}MC state in the ISC process, intriguingly shows very little effects of halogenation on the rocking PESs, with each PES showing no preference for rocking and overall similar curvatures.

The current computational results were also used to evaluate previous hypotheses about why heavier halogens showed longer lifetimes than when lighter halogens were used as substituents. Prior interpretations assumed that using heavier halogens decreased the driving force and/or increased the reorganization energy involved in the $^{5/7}$MLCT to ^{3}MC conversion, thereby slowing the rate of ISC down. DFT calculations provided a different picture, with the driving force for the ^{7}MLCT to ^{3}MC step being less favorable for the fluorinated complex than the complexes where heavier halogens were used. This trend can still explain the shorter lifetime of the fluorinated complex, however, as the calculations also show that for all the halogenated complexes the ^{7}MLCT to ^{3}MC conversion belongs in the Marcus "inverted" region and therefore any increases in driving force will actually lead to a decrease in reaction rates. Alternatively, the decrease in reaction rate can be explained by the energy gap law, which also predicts a decrease in reaction rates as the states become further separated in energy. Overall this study provided some alternative hypotheses on the ISC process for this system, but also demonstrated the need for more sophisticated, multi-dimensional PES studies on these systems to further understand the factors that affect excited state lifetimes.

Conflicts of interest

There are no conflicts to declare.

Acknowledgements

This work was supported by the National Science Foundation grant CHE-1554855. Additionally, we acknowledge the use of the computing resources of the High-Performance Computing Center at NCSU.

References

1. D. C. Ashley and E. Jakubikova, *Coord. Chem. Rev.*, 2017, **337**, 97-111.
2. A. Bousseksou, G. Molnár and G. Matouzenko, *Eur. J. Inorg. Chem.*, 2004, **2004**, 4353-4369.
3. A. B. Gaspar, V. Ksenofontov, M. Seredyuk and P. Gütlich, *Coord. Chem. Rev.*, 2005, **249**, 2661-2676.
4. T. G. Gopakumar, F. Matino, H. Naggert, A. Bannwarth, F. Tuczek and R. Berndt, *Angew. Chem. Int. Ed.*, 2012, **51**, 6262-6266.
5. I. Žutić, J. Fabian and S. Das Sarma, *Rev. Mod. Phys.*, 2004, **76**, 323-410.
6. E. Jakubikova and D. N. Bowman, *Acc. Chem. Res.*, 2015, **48**, 1441-1449.
7. B. O'Regan and M. Gratzel, *Nature*, 1991, **353**, 737-740.
8. A. Hagfeldt, G. Boschloo, L. Sun, L. Kloo and H. Pettersson, *Chem. Rev.*, 2010, **110**, 6595-6663.
9. S. Ferrere and B. A. Gregg, *J. Am. Chem. Soc.*, 1998, **120**, 843-844.
10. S. Ferrere, *Chem. Mater.*, 2000, **12**, 1083-1089.
11. S. Ferrere, *Inorg. Chim. Acta*, 2002, **329**, 79-92.
12. J. E. Monat and J. K. McCusker, *J. Am. Chem. Soc.*, 2000, **122**, 4092-4097.
13. W. Zhang, R. Alonso-Mori, U. Bergmann, C. Bressler, M. Chollet, A. Galler, W. Gawelda, R. G. Hadt, R. W. Hartsock, T. Kroll, K. S. Kjaer, K. Kubicek, H. T. Lemke, H. W. Liang, D. A. Meyer, M. M. Nielsen, C. Purser, J. S. Robinson, E. I. Solomon, Z. Sun, D. Sokaras, T. B. van Driel, G. Vanko, T. C. Weng, D. Zhu and K. J. Gaffney, *Nature*, 2014, **509**, 345-348.
14. E. A. Juban, A. L. Smeigh, J. E. Monat and J. K. McCusker, *Coord. Chem. Rev.*, 2006, **250**, 1783-1791.
15. C. Bressler, C. Milne, V.-T. Pham, A. ElNahhas, R. M. van der Veen, W. Gawelda, S. Johnson, P. Beaud, D. Grolimund, M. Kaiser, C. N. Borca, G. Ingold, R. Abela and M. Chergui, *Science*, 2009, **323**, 489-492.
16. W. Zhang and K. J. Gaffney, *Acc. Chem. Res.*, 2015, **48**, 1140-1148.
17. J. K. McCusker, *Nat. Phys.*, 2014, **10**, 476-477.
18. A. Moguilevski, M. Wilke, G. Grell, S. I. Bokarev, S. G. Aziz, N. Engel, A. A. Raheem, O. Kühn, I. Y. Kiyan and E. F. Aziz, *Chem. Phys. Chem.*, 2017, **18**, 465-469.
19. C. D. Graaf and C. Sousa, *Int. J. Quantum Chem.*, 2011, **111**, 3385-3393.
20. J. Chang, A. Fedro and M. van Veenendaal, *Phys. Rev. B*, 2010, **82**.
21. M. van Veenendaal, J. Chang and A. J. Fedro, *Phys. Rev. Lett.*, 2010, **104**.
22. M. Pápai, G. Vankó, C. de Graaf and T. Rozgonyi, *J. Chem. Theory Comput.*, 2013, **9**, 509-519.
23. A. Rudavskyi, C. Sousa, C. de Graaf, R. W. Havenith and R. Broer, *J. Chem. Phys.*, 2014, **140**, 184318.
24. D. C. Ashley and E. Jakubikova, *Inorg. Chem.*, 2018, **57**, 5585-5596.
25. K. F. Purcell, *J. Am. Chem. Soc.*, 1979, **101**, 5147-5152.
26. L. G. Vanquickenborne and K. Pierloot, *Inorg. Chem.*, 1981, **20**, 3673-3677.
27. E. B. Fleischer, A. E. Gebala, D. R. Swift and P. A. Tasker, *Inorg. Chem.*, 1972, **11**, 2775-2784.
28. R. A. D. Wentworth, *Coord. Chem. Rev.*, 1972, **9**, 171-187.
29. P. Comba, A. M. Sargeson, L. M. Engelhardt, J. M. Harrowfield, A.

H. White, E. Horn and M. R. Snow, *Inorg. Chem.*, 1985, **24**, 2325-2327.
30. P. Comba, *Inorg. Chem.*, 1989, **28**, 426-431.
31. J. K. McCusker, A. L. Rheingold and D. N. Hendrickson, *Inorg. Chem.*, 1996, **35**, 2100-2112.
32. S. Alvarez, *J. Am. Chem. Soc.*, 2003, **125**, 6795-6802.
33. E. Cremades, J. Echeverría and S. Alvarez, *Chem. Eur. J.*, 2010, **16**, 10380-10396.
34. J. C. Knight, S. Alvarez, A. J. Amoroso, P. G. Edwards and N. Singh, *Dalton Trans.*, 2010, **39**, 3870-3883.
35. S. Alvarez, *Chem. Rev.*, 2015, **115**, 13447-13483.
36. P. Stock, E. Deck, S. Hohnstein, J. Korzekwa, K. Meyer, F. W. Heinemann, F. Breher and G. Horner, *Inorg. Chem.*, 2016, **55**, 5254-5265.
37. C. D. Montgomery and C. J. Shorrock, *Inorg. Chim. Acta*, 2002, **328**, 259-262.
38. F. Renz, H. Oshio, V. Ksenofontov, M. Waldeck, H. Spiering and P. Gütlich, *Angew. Chem. Int. Ed.*, 2000, **39**, 3699-3700.
39. A. Hauser, C. Enachescu, M. L. Daku, A. Vargas and N. Amstutz, *Coord. Chem. Rev.*, 2006, **250**, 1642-1652.
40. S. E. Canton, X. Zhang, M. L. Lawson Daku, Y. Liu, J. Zhang and S. Alvarez, *J. Phys. Chem. C*, 2015, **119**, 3322-3330.
41. E. C. Constable, G. Baum, E. Bill, R. Dyson, R. van Eldik, D. Fenske, S. Kaderli, D. Morris, A. Neubrand, M. Neuburger, D. R. Smith, K. Wieghardt, M. Zehnder and A. D. Zuberbühler, *Chem. Eur. J.*, 1999, **5**, 498-508.
42. G. A. Craig, O. Roubeau and G. Aromí, *Coord. Chem. Rev.*, 2014, **269**, 13-31.
43. L. J. Kershaw Cook, R. Mohammed, G. Sherborne, T. D. Roberts, S. Alvarez and M. A. Halcrow, *Coord. Chem. Rev.*, 2015, **289-290**, 2-12.
44. J. M. Holland, J. A. McAllister, C. A. Kilner, M. Thornton-Pett, A. J. Bridgeman and M. A. Halcrow, *J. Chem. Soc., Dalton Trans.*, 2002, 548-554.
45. S. Vela, J. J. Novoa and J. Ribas-Arino, *Phys. Chem. Chem. Phys.*, 2014, **16**, 27012-27024.
46. S. Y. Brauchli, E. C. Constable, K. Harris, D. Häussinger, C. E. Housecroft, P. J. Rösel and J. A. Zampese, *Dalton Trans.*, 2010, **39**, 10739-10748.
47. L. J. Kershaw Cook, F. L. Thorp-Greenwood, T. P. Comyn, O. Cespedes, G. Chastanet and M. A. Halcrow, *Inorg. Chem.*, 2015, **54**, 6319-6330.
48. J. Nance, D. N. Bowman, S. Mukherjee, C. T. Kelley and E. Jakubikova, *Inorg. Chem.*, 2015, **54**, 11259-11268.
49. S. G. Shepard, S. M. Fatur, A. K. Rappe and N. H. Damrauer, *J. Am. Chem. Soc.*, 2016, **138**, 2949-2952.
50. S. M. Fatur, S. G. Shepard, R. F. Higgins, M. P. Shores and N. H. Damrauer, *J. Am. Chem. Soc.*, 2017, **139**, 4493-4505.
51. Y. Li, X.-W. Fan, J. Chen, F.-Q. Bai and H.-X. Zhang, *RSC Advances*, 2019, **9**, 31621-31627.
52. C. Sousa, C. de Graaf, A. Rudavskyi, R. Broer, J. Tatchen, M. Etinski and C. M. Marian, *Chem. Eur. J.*, 2013, **19**, 17541-17551.
53. A. D. Becke, *Phys. Rev. A*, 1988, **38**, 3098-3100.
54. A. D. Becke, *J. Chem. Phys.*, 1993, **98**, 5648-5652.
55. A. D. Becke, *J. Chem. Phys.*, 1993, **98**, 1372-1377.
56. C. Lee, W. Yang and R. G. Parr, *Phys. Rev. B*, 1988, **37**, 785-789.
57. S. Grimme, *J. Comput. Chem.*, 2006, **27**, 1787-1799.
58. D. N. Bowman, A. Bondarev, S. Mukherjee and E. Jakubikova, *Inorg. Chem.*, 2015, **54**, 8786-8793.
59. M. Reiher, *Inorg. Chem.*, 2002, **41**, 6928-6935.
60. O. Salomon, M. Reiher and B. A. Hess, *J. Chem. Phys.*, 2002, **117**, 4729-4737.
61. M. Reiher, O. Salomon and B. Artur Hess, *Theor. Chem. Acc.*, 2001, **107**, 48-55.
62. M. Dolg, U. Wedig, H. Stoll and H. Preuss, *J. Chem. Phys.*, 1987, **86**, 866-872.
63. A. Bergner, M. Dolg, W. Küchle, H. Stoll and H. Preuß, *Mol. Phys.*, 1993, **80**, 1431-1441.
64. R. Krishnan, J. S. Binkley, R. Seeger and J. A. Pople, *J. Chem. Phys.*, 1980, **72**, 650-654.
65. M. J. Frisch, G. W. Trucks, H. B. Schlegel, G. E. Scuseria, M. A. Robb, J. R. Cheeseman, G. Scalmani, V. Barone, B. Mennucci, G. A. Petersson, H. Nakatsuji, M. Caricato, X. Li, H. P. Hratchian, A. F. Izmaylov, J. Bloino, G. Zheng, J. L. Sonnenberg, M. Hada, M. Ehara, K. Toyota, R. Fukuda, J. Hasegawa, M. Ishida, T. Nakajima, Y. Honda, O. Kitao, H. Nakai, T. Vreven, J. A. Montgomery, Jr., J. E. Peralta, F. Ogliaro, M. Bearpark, J. J. Heyd, E. Brothers, K. N. Kudin, V. N. Staroverov, R. Kobayashi, J. Normand, K. Raghavachari, A. Rendell, J. C. Burant, S. S. Iyengar, J. Tomasi, M. Cossi, N. Rega, N. J. Millam, M. Klene, J. E. Knox, J. B. Cross, V. Bakken, C. Adamo, J. Jaramillo, R. Gomperts, R. E. Stratmann, O. Yazyev, A. J. Austin, R. Cammi, C. Pomelli, J. W. Ochterski, R. L. Martin, K. Morokuma, V. G. Zakrzewski, G. A. Voth, P. Salvador, J. J. Dannenberg, S. Dapprich, A. D. Daniels, Ö. Farkas, J. B. Foresman, J. V. Ortiz, J. Cioslowski and D. J. Fox, *Journal*, 2009.
66. L. M. Lawson Daku, F. Aquilante, T. W. Robinson and A. Hauser, *J. Chem. Theory Comput.*, 2012, **8**, 4216-4231.
67. A. Vargas, I. Krivokapic, A. Hauser and L. M. Lawson Daku, *Phys. Chem. Chem. Phys.*, 2013, **15**, 3752-3763.
68. E. Papajak and D. G. Truhlar, *J. Chem. Theory Comput.*, 2011, **7**, 10-18.
69. D. N. Bowman and E. Jakubikova, *Inorg. Chem.*, 2012, **51**, 6011-6019.
70. R. A. Marcus, *J. Chem. Phys.*, 1956, **24**, 966-978.
71. J. R. Bolton and M. D. Archer, in *Electron Transfer in Inorganic, Organic, and Biological Systems*, American Chemical Society, 1991, vol. 228, ch. 2, pp. 7-23.
72. N. Sutin, *Acc. Chem. Res.*, 1982, **15**, 275-282.
73. G. Basu, A. Kitao, A. Kuki and N. Go, *J. Phys. Chem. B*, 1998, **102**, 2076-2084.
74. S. F. Nelsen, S. C. Blackstock and Y. Kim, *J. Am. Chem. Soc.*, 1987, **109**, 677-682.
75. O. López-Estrada, H. G. Laguna, C. Barrueta-Flores and C. Amador-Bedolla, *ACS Omega*, 2018, **3**, 2130-2140.
76. S. Chaudhuri, S. Hedström, D. D. Méndez-Hernández, H. P. Hendrickson, K. A. Jung, J. Ho and V. S. Batista, *J. Chem. Theory Comput.*, 2017, **13**, 6000-6009.
77. K. M. Rosso and M. Dupuis, *Theor. Chem. Acc.*, 2006, **116**, 124-136.
78. E. Laborda, M. C. Henstridge, C. Batchelor-McAuley and R. G. Compton, *Chem. Soc. Rev.*, 2013, **42**, 4894-4905.
79. J. Wu, M. Alías and C. de Graaf, *Inorganics*, 2020, **8**.
80. E. M. Kober, J. V. Caspar, R. S. Lumpkin and T. J. Meyer, *J. Phys. Chem.*, 1986, **90**, 3722-3734.
81. C. M. Marian, *WIREs Comput. Mol. Sci.*, 2012, **2**, 187-203.